Structural Changes and Development of Transport Properties During the Conversion of a Polyimide Membrane to a Carbon Membrane

Aik Chong Lua, Jincai Su

Division of Thermal and Fluids Engineering, School of Mechanical and Aerospace Engineering, Nanyang Technological University, Singapore 639798, Republic of Singapore

Received 30 March 2007; accepted 29 November 2008
DOI 10.1002/app.29841
Published online 16 March 2009 in Wiley InterScience (www.interscience.wiley.com).

ABSTRACT: Kapton®100HN polyimide membranes were heat treated at temperatures ranging from 623 to 1073 K. The precursor and the heat-treated membranes were characterized by thermogravimetric analysis, X-ray diffraction, Raman spectroscopy, density measurement, nitrogen adsorption at 77 K, and single gas permeation. Compared with the precursor, the X-ray diffraction patterns did not change greatly when the membranes were heat treated at 623–748 K. The membranes treated at 623–723 K showed similar gas permeation rates as the original polyimide membrane whereas those treated at 773–873 K showed remarkable increases in the gas permeances due to the decomposition of the polyimide. Two minimum ideal selectivities were found for the membranes treated at 673 and 723 K. An increase in the temperature from 873 to 1073 K increased the crystallinity and decreased the interplanar spacing in the carbon membranes which had microporous structures as shown by their Type I adsorption isotherms. The membranes treated at 773 K were deemed to be at an intermediate stage between polymer and amorphous carbon. By increasing the temperature from 773 to 873 K, the polyimide changed to a carbon membrane. The gas permeances for He, CO_2, O_2,N_2, and CH_4 were increased from 1.06×10^{-9}, 1.10×10^{-9}, 1.90×10^{-10}, 5.70×10^{-11}, and 5.55×10^{-11} to 2.68×10^{-8}, 3.62×10^{-8}, 9.98×10^{-9}, 1.66×10^{-9}, and 5.17×10^{-10} mol/(m^2 s Pa), respectively. J Appl Polym Sci 113: 235–242, 2009

Key words: polyimide; heat treatment; gas permeation; structure; carbon membrane

INTRODUCTION

Carbon molecular sieve membranes have been intensively studied for the past few years as a promising candidate for gas separations.[1,2] These membranes are porous with pores approaching the molecular dimensions of the gas molecules. They have comparable or even higher permselectivity and permeation properties as well as thermal and chemical stability than polymeric and other microporous inorganic membranes. Carbon molecular sieve membranes are prepared by the carbonization of polymeric substances (hollow fiber or thin polymeric films) or the carbonization of films deposited on macro- or mesoporous supports (carbon disks, ceramic plates or tubes, stainless steel tubes, and alumina tubes) by brush-coating, spray-coating, dip-coating, or ultrasonic deposition techniques.[3–5] Factors such as (1) the choice of polymer precursor, (2) the membrane formation method, and (3) the pyrolysis process are believed to significantly affect the microstructure and gas separation properties of the resulting carbon membranes.[6]

Polyimides have been widely used to prepare carbon molecular sieve membranes. Geiszler and Koros prepared hollow fiber carbon membranes from polyimide. The effects of pyrolysis parameters such as the pyrolysis atmosphere, the final temperature, the purge gas flow rate as well as the residual oxygen in the inert purge gas were studied.[7] It was observed that pyrolysis in an inert atmosphere enhanced the degradation process due to the increased mass and heat transfer as compared with pyrolysis under vacuum. The effect of the purge gas flow rate would affect the gas permeation rate because the membrane pores might be blocked by carbon deposited from the polyimide decomposition byproducts and this phenomenon was more pronounced when the pyrolysis was carried out at low temperatures. The pyrolysis temperature was found to significantly influence the membrane properties by affecting (1) the pyrolysis kinetics of the polyimide, (2) the pyrolysis kinetics of the polyimide degradation byproducts, and (3) the compactness of the turbostratic carbon structure. Tin et al. produced carbon molecular sieve membranes from chemically modified and solvent

Correspondence to: A. C. Lua (maclua@ntu.edu.sg).

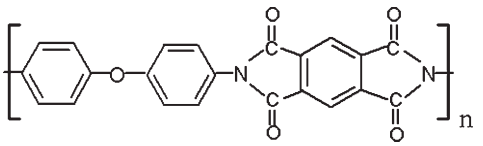

Figure 1 Structure of Kapton® polyimide.

treated polyimides.[8] Before pyrolysis under vacuum at 1073 K, the membranes prepared from Matrimid® polyimide with a thickness of 60 μm were modified through either crosslinking by immersing them into a *p*-xylenediamine/methanol reagent for specific durations or solvent treatment by immersing them into pure methanol. The gas permeation rate of the carbon membranes from the crosslinked Matrimid polyimide decreased with increasing crosslinking density while the maximum ideal separation factor was achieved from the 1-day crosslinked Matrimid polyimide. Methanol treatment of the precursor significantly increased the carbon membrane selectivity due to the induced chain mobility and the increased interstitial space among the Matrimid chains.

Fuertes et al. obtained microporous carbon composite membranes from two commercial polyimides: Matrimid5218 and Allotherm®610-16.[2] The preparation procedures involved (1) coating of the macroporous carbon supports with the polymeric solution, (2) gellation of the resulting polymeric films by immersion into a coagulant bath following the phase inversion technique, and (3) heat treatment (723–973 K) of the polymeric membranes under vacuum. The resulting carbon membranes showed ideal selectivities of 46–24, 5.9–2.9 and 32.9–5.4 for He/N_2, O_2/N_2 and CO_2/CH_4, respectively, with permeabilities of 9–69, 1–7 and 2–12 Barrers for He, O_2 and CO_2, respectively. They found that the carbon membranes from Allotherm® polyimide were more permeable and less selective than those from Matrimid polyimide. Barsema et al. found that the structure of Matrimid polyimide changed to an intermediate state upon heat treatment at 623–698 K for 5–30 min under nitrogen and then to carbon after pyrolysis at higher temperatures.[9] All the samples tested were pretreated at 623 K for 120 min for the removal of any thermal and physical history. It was observed that the infra-red adsorption intensities decreased with a more intense heat treatment. When treated at temperatures from 623 to 698 K, the samples were still dense polymeric membranes and showed slightly increased densities and decreased gas permeabilities for O_2 and N_2 as compared to the pretreated samples. The increasing formation of charge transfer complexes (CTCs) as well as the densification of the polymer structure upon heat treatment above the glass transition temperature might be the reason for these phenomena. Heat treatment at 773 K or higher temperatures led to significant increase in the membrane density due to the onset of carbonization and the resulting membranes exhibited exponentially increased gas permeabilities. The membranes heat treated at 748 K exhibited properties of an intermediate state between polymeric membrane and carbon membrane and showed sharp increases in the CO_2, O_2 and N_2 permeabilities over the polymeric membrane.

Shao et al. studied the evolution of the physicochemical and transport properties of 6FDA-durene to carbon membrane.[10] During the heat treatment of the polymeric membranes at 598–1073 K under vacuum, the imide characteristic peaks (C=O asymmetric stretching at 1786 cm^{-1}, C=O symmetric stretching at 1716 cm^{-1} and C—N stretching of imide groups at 1351 cm^{-1}) that were found to stay intact below 723 K changed remarkably when the temperature was raised above 723 K. The scission of CF_3 dominated in the intermediate stage (673–773 K) while the degradation and transformation of imide groups dominated in the early stage of the carbonization process. Simultaneously, the 6FDA-durene changed from the original amorphous state to an intermediate state at 723–773 K and then to carbon molecular sieve membrane at higher temperatures. The change of 6FDA-durene to carbon membrane upon heat treatment improved the ideal selectivities from 8.84 to 79.9 for He/N_2 and from13.6 to 137 for CO_2/CH_4, respectively.

In this paper, commercial polyimide Kapton®100HN was used as a precursor to study the evolution of the membrane structure and the transport properties from polymer to an intermediate state and then finally to carbon membrane during heat treatment. The weight change of Kapton100HN during heat treatment was determined by thermogravimetric analysis; the change in the transport properties was studied through single gas permeation tests; and the pore structure of the carbonized membranes was analyzed by N_2 (77 K) adsorption and Raman spectroscopy.

EXPERIMENTAL

Membrane preparation

All membranes described in this study were prepared by heat treatment of a commercially available Kapton100HN polyimide film. The Kapton film with a thickness of 25 μm was synthesized by polymerizing an aromatic dianhydride and an aromatic diamine. The film has excellent chemical resistance with no known organic solvents for it. The structure of the Kapton polyimide is given in Figure 1. The heat treatment of the Kapton film was carried out in a tube furnace system which was given in a previous

paper.[11] The Kapton film was cut into circular pieces with diameters around 30 mm. These circular films, located between porous graphite discs, were placed inside the horizontal stainless-steel reactor (length of 950 mm and diameter of 70 mm) which was then put at the center of the horizontal furnace (CTF 12/75/700, Carbolite, UK). During heat treatment, nitrogen was passed through the reactor at a flow rate of 100 mL/min. Before the heat treatment or pyrolysis process, the whole system was purged with nitrogen for 1 h. For the membranes carbonized at temperatures of 773 K or less, the polyimide film was subjected to a heating rate of 5 K/min and held at that temperature for 1 h. Otherwise, for the high-temperature carbonized membranes, the polyimide membranes were firstly heated to 673 K at a heating rate of 5 K/min and subjected to a thermal soak time of 1 h, and then finally heated to the required temperature at a heating rate of 0.5 K/min with a thermal soak time of 2 h at the final temperature. The membranes after heat treatment were cooled to the ambient temperature at a rate of 2 K/min.

Characterization of the heat-treated membranes

A thermogravimetric (TG) analyzer (DTA60, Shimadzu, Japan) was used to determine the membrane weight loss during the pyrolysis process. Small pieces of the Kapton film weighing about 2 mg were placed onto the aluminum pan of the analyzer. The TG experiments were carried out under a nitrogen (99.9995% pure) flow of 50 mL/min. During pyrolysis, the samples were heated from room temperature to 673 K at a heating rate of 5 K/min with a thermal soak time of 1 h at this temperature and then heated at different rates of 0.5, 2, 4, 6 and 10 K/min to a final temperature of 1123 K, followed by cooling to the ambient temperature.

An ultrapycnometer (1000, Quantachrome, USA) was used to determine the true density of the precursor and the heat-treated membranes. These tests were performed at 295 ± 1 K using He as the analysis gas.

Wide angle X-ray diffraction (XRD) was used to study the structure of the polyimide precursor and the membranes heat treated at various temperatures. The tests were carried out using a X-ray diffractometer (PW1830, Philips, Netherlands) with Cu-Kα radiation of 1.54 Å. The X-ray generator operates at 40 kV and 30 mA with a step size of 0.02°. The average *d*-spacing of the pyrolysed membranes was estimated using Bragg's law, i.e.,

$$n\lambda = 2d \sin \theta \tag{1}$$

where n is the order of reflection, λ is the wavelength of X-ray (1.5405 Å, Cu), d is the interplanar spacing of the (002) plane, and θ is the diffraction angle.

Raman spectroscopy (1000, Renishaw, UK) was used to study the structure of the membranes heat treated at 873 and 1073 K. A HeNe laser was used to emit an intense laser beam with a fixed wavelength (632.8 nm). The emitted laser light passed through a lens and was focused on the membrane sample through a 50× magnification lens. The scattered Raman light was collected and a plot of photon intensity (count) versus the wavenumber shift from the laser line was obtained. Raman spectra were routinely acquired in the range from 800 to 2000 cm^{-1} using a 1800 lines/mm grating.

Membrane structure analysis

The structural characteristics are useful to understand the mechanism and efficiency of the carbonized membranes for gas separation. N_2 (77 K) adsorption experiments were performed using an accelerated surface area and porosimetry system (ASAP2010, Micromeritics). To eliminate possible problems arising from helium entrapment inside the micropores during free-space measurements, the tests were always stopped after obtaining the free-space and the samples were degassed again overnight at 573 K before analysis.

Pure gas permeation

Permeances of four gases with their molecular diameters in parentheses, viz., CO_2 (3.3 Å), O_2 (3.46 Å), He (2.6 Å), and N_2 (3.64 Å) were measured at 295 ± 1 K using a high-vacuum time-lag method at a feed pressure of 1 atm absolute at 295 ± 1 K. Before each test, a membrane was attached to the permeation cell and both sides were evacuated to 10^{-5} Torr vacuum using an oil-free molecular vacuum pump (1025, Alcatel, France. The feed pressure (P_H^0) was measured using a differential pressure transducer (DP15, Validyne, USA) and maintained at a constant value of 1 atm during the test. The variation of the downstream pressure was detected by a high-resolution absolute pressure transducer (627B, 10 Torr, MKS, USA). The pure gas permeability $\overline{P}_i^0$ for the component i through the membrane is defined by[12]:

$$\ln\left[\frac{P_H^0 - P_L^*}{P_H^0 - P_L(t)}\right] = A \cdot \frac{\overline{P}_i^0}{l} \cdot \frac{RT}{V_L} \cdot (t - t^*) \tag{2}$$

where P_H^0 is the feed pressure, t^* is a certain period of time needed to attain a constant pressure in the high pressure side, t is the time required to attain a pressure $P_L(t)$ at the low pressure side, P_L^* is the pressure before each test at the low pressure side, A is the surface area of the membrane, and V_L is the

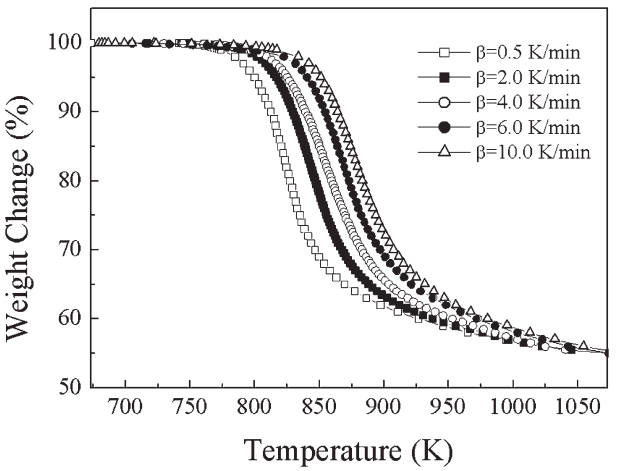

Figure 2 Thermogravimetric curves on the pyrolysis of Kapton® 100HN under nitrogen.

calibrated volume of the low pressure side. A plot of $\ln[(P_H^0 - P_L^*)/(P_H^0 - P_L(t))]$ versus $(t - t^*)$ should give a straight line from which the permeability could be obtained. The thickness of the membrane, which is required for the determination of the permeability, is not readily measurable; therefore, the gas permeance $(\overline{P}_i^0/l)$ is used instead in this study to represent the permeation rate of the single gas.

RESULTS AND DISCUSSION

Thermogravimetric analysis

Changes in the relative weight with heat-treatment temperatures for the Kapton100HN polyimide film for various heating rates are shown in Figure 2. The color of the film when subjected to heat treatment changed from transparent yellow to dark brown and then to black due to pyrolysation and the films heat treated above 773 K showed appreciable shrinkage. The pyrolysis of the Kapton100HN polyimide covered a wide range of temperatures and the various runs carried out under different heating rates produced nearly the same percent of residues at the final temperature (Fig. 2). The decomposition begins around 773 K and the sample weight decreases significantly within a narrow temperature range of 773–923 K with the evolution of mainly CO and CO_2 as the gaseous products. Beyond this temperature range, the weight change eases, resulting in gradual decreases with increasing temperature due to the evolution of CH_4, H_2, and N_2.[13–15] The TG curves shift to the right-hand side with increasing heating rate, resulting in a faster time to reach a certain temperature, and hence a lesser amount of volatiles are released. It has been reported that these weight changes are related to the activation energy of the pyrolysis reaction.[16] According to Jones and Koros, heat treatment at higher temperatures will lead to a higher crystallinity, higher density, and a narrower interplanar spacing of the pyrolysed carbon.[17] Pyrolysis at high temperature with low heating rate and long soak time is needful to minimize the effective pores but increases the possibility of the formation of cracks in the resulting carbon membranes.

X-ray diffraction spectra

In the XRD experiments, the angle 2θ was swept from 10° to 50°. Figure 3 shows the XRD spectra of the polyimide membrane and the membranes heat treated at various temperatures. The X-ray spectrum of the polyimide membrane displays three main characteristic reflections with the peaks at 2θ = 15.10°, 22.44°, and 26.12°, with the most intense peak appearing at 2θ = 22.44°. This diffraction pattern elucidates the semicrystalline nature of the Kapton polyimide. The membranes heat treated at low temperatures (623–748 K) show very similar X-ray diffraction patterns to that of the original polyimide membrane. However, the pyrolysed membranes exhibit more distinct peaks, indicating increased crystallinity over the precursor. The broad asymmetric peaks at 2θ = 23.78° and 23.98° shown by the spectra for 873 and 1073 K are typical of amorphous carbon and the peaks may be ascribed to disordered graphitic 002 planes. With increasing heat-treatment temperature from 873 to 1073 K, the 002 peak shifting to higher degree verifies narrowing of the interplanar spacing and the development of increased crystallinity. The average *d*-spacing values for the two samples at 873 and 1073 K determined by Bragg's equation are 3.74 and 3.71 Å, respectively. The membrane heat treated at 773 K gives a broad peak at 2θ = 22.54° with an average *d*-spacing of 3.94 Å; its pattern is similar to those of membranes heat treated at 873 and 1073 K. The sample heat

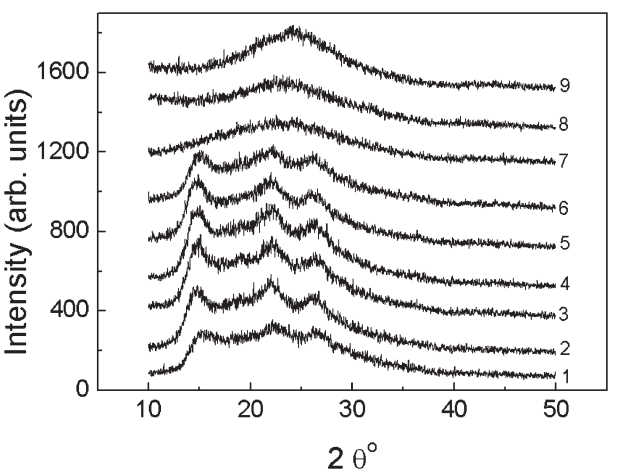

Figure 3 X-ray diffraction spectra for the polyimide membrane (1), and the membranes heat treated at 623, 673, 698, 723, 748, 773, 873, and 1073 K (2–9).

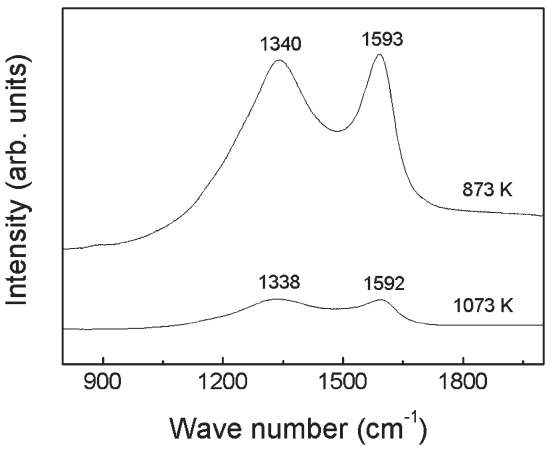

Figure 4 Raman spectra of the membranes heat treated at 873 and 1073 K.

treated at 773 K is at the particular temperature whereby the decomposition of the Kapton polyimide has just begun as seen from the TG analysis in Figure 2. Thus, the membrane at 773 K possesses certain properties of polymer membrane as well as amorphous carbon membrane. This unique property may be an intermediate state between polymer and carbon as suggested by Barsema et al.[9] and Shao et al.[10]

Raman spectra

Amorphous carbon film usually gives two peaks in the Raman spectrum: the G-peak around 1580 cm^{-1} and the D-peak around 1350 cm^{-1}. The G-peak is the Raman active E_{2g_2} mode of graphite involving the in-plane bond-stretching motion of sp^2-hybridized C atoms while the D-peak is a breathing mode of A_{1g} symmetry involving phonons near the K zone boundary.[18–20] As shown in Figure 4, the G-peaks at 1593 cm^{-1} and 1592 cm^{-1} and the D-peaks at 1340 cm^{-1} and 1338 cm^{-1} can be found in the Raman spectra of the membranes heat treated at 873 and 1073 K, respectively. The G-peak and the D-peak for the two samples are broad and overlapping occurs, resulting in smaller separation of the two spectral components due to the laser excitation wavelength. With increasing heat-treatment temperature from 873 to 1073 K, the carbon membranes show marked decreases in the absorption peak intensity of the G-peak and D-peak. These carbon membranes are amorphous based on the Raman spectra patterns because the D mode is invisible in perfect graphite and only becomes active in the presence of disorder.[20] The intensities of the G-peak (I_G) and the D-peak (I_D) were estimated from the two-peak Gaussian curve fitting. A decrease in the I_D/I_G ratio based on the peak width from 2.51 to 2.46 was shown on the spectra for the membranes heat treated at 873 and 1073 K, respectively. The I_D/I_G ratio can be used to determine the in-plane size of the graphitic clusters (L_a) using the Tuinstra-Koenig relation:

$$L_a(\text{nm}) = C(\lambda)(I_D/I_G)^{-1} \quad (3)$$

where $C(\lambda)$ is a constant related to the wave length of the laser which is determined using the method developed by Matthews et al.[21] The calculated values of L_a for the membranes heat treated at 873 and 1073 K are 3.30 and 3.36 nm, respectively. Based on the L_a values and the peak positions, these two samples may have nanocrystalline graphitic structures with graphitic cluster diameters of 3.30 and 3.36 nm. As the increase of the L_D/I_G ratio is inversely proportional to the crystalline size for the disordered graphite and sp^3/sp^2 ration in the amorphous carbon, a more "ordered" structure and increased sp^2 content in the pyrolysed samples are obtained with increasing heat-treatment temperature from 873 to 1073 K.[22]

Structural analysis of the carbon membranes

Figure 5 shows the N_2 (77 K) adsorption isotherms of the carbon membranes heat treated at 873 and 1073 K. The isotherms are characterized by abrupt increases in the low-pressure region and then become flat with increasing relative pressure. The N_2 (77 K) adsorption isotherm of the membrane heat treated at 1073 K shows an upsurge as the saturation pressure approaches. Both isotherms are typical Type I isotherms which are associated with solids containing micropores no more than a few molecular diameters in width.[23] The carbon membrane obtained at 873 K shows higher nitrogen uptake than the membrane obtained at 1073 K, indicating the existence of more pores available for nitrogen adsorption in the former. With increasing heat-

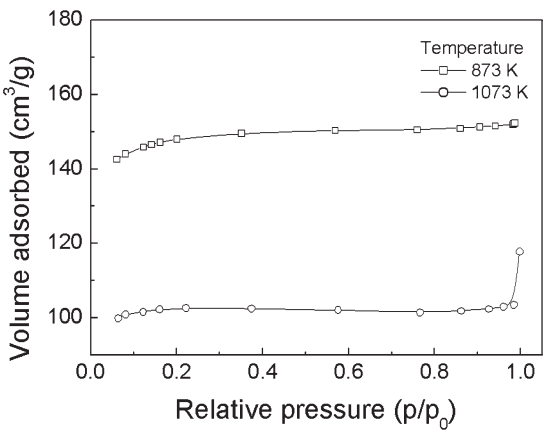

Figure 5 N_2 adsorption isotherms of the membranes heat treated at 873 and 1073 K.

TABLE I
Pore Structural Properties of Carbon Membranes Heat Treated at 873 and 1073 K

Temperature (K)	BET surface area (m^2/g)	Total pore volume (cm^3/g)	Micropore volume (cm^3/g)
873	497.61	0.2354	0.1974
1073	334.29	0.1823	0.1464

treatment temperature from 873 to 1073 K, the BET surface area, the micropore volume and the total pore volume decrease from 497.61 m^2/g, 0.1974 cm^3/g, and 0.2354 cm^3/g to 334.29 m^2/g, 0.1464 cm^3/g, and 0.1823 cm^3/g, respectively (Table I). An examination of the TG curve (Fig. 2) for a heating rate of 0.5 K/min shows that the decomposition of the precursor commences at about 773 K with a maximum weight loss rate occurring at about 825 K. The rate of pyrolysis reaction is very high for the temperature range of 773–873 K, but slowing down after 873 K. The maximum decomposition rate at about 825 K usually results in the maximum rate of pore formation. Hence, in Figure 5 and Table I, for a pyrolysis temperature of 873 K and a hold time of 2 h, a large amount of pores including micropores and mesopores are created. Further increase in the heat treatment temperature to 1073 K with the same thermal soak time of 2 h results in significant shrinkage of the existing pores although a certain amount of new pores are generated by this pyrolysis reaction. On the whole, at this higher pyrolysis temperature, the pores accessible to nitrogen adsorption significantly decrease. Figure 6 shows the pore size distributions of the carbon membranes heat treated at 873 and 1073 K using a density functional theory (DFT) software (V2.02, Micromeritics). For the 873 K carbon membrane, a comparatively high proportion of pore size between 20 and 30 Å was detected while

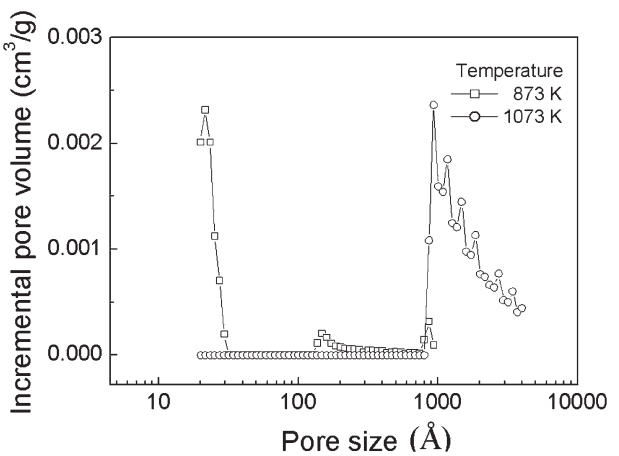

Figure 6 Pore size distributions determined from N_2 adsorption data using DFT method for the membranes heat treated at 873 and 1073 K.

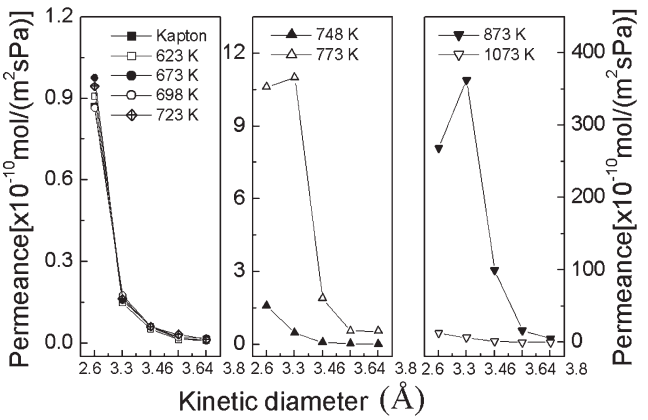

Figure 7 Pure gas permeances for the polyimide membrane and the membranes heat treated at temperatures in the range of 623–1073 K.

none was detected for the 1073 K carbon membrane in the same range. It could be surmised that the latter membrane could have shrunk with high temperature heat treatment. Pore sizes less than 20 Å could not be detected by the normal N_2 adsorption at 77 K. Pore sizes greater than 800 Å appeared for the 1073 K carbon membrane; this could possibly be attributed to the formation of crevices or cracks due to the membrane shrinkage at this high pyrolysis temperature.

Gas permeation properties of membranes heat treated at different temperatures

The effect of heat treatment on the membrane transport properties is shown in Figure 7. The changes in the gas permeance with the kinetic diameter of the various penetrating gas molecules are indicative of the degree of molecular sieving property of these membranes. The membranes heat treated at 623, 673, 698, and 723 K show very low and comparable gas permeances for all the gases tested. A heat-treatment temperature of 748 K results in an increase in the gas permeance despite that this membrane shows similar XRD pattern to those of the membranes subjected to lower temperatures (Fig. 3). Further increases in the heat-treatment temperature to 773 and 873 K result in significant increasing gas permeation rate. However, the membrane heat treated at 1073 K show very low gas permeance, indicating a dramatic change in the pore structure as compared to that of the membrane heat treated at 873 K. This significant decrease in the gas permeance lends support to the earlier thesis of membrane shrinkage with reference to Figure 6. Overall, the change in the gas permeance with the heat-treatment temperature is consistent with the results of the TG analysis: the decomposition of the Kapton® polyimide commences around 773 K which coincides with the

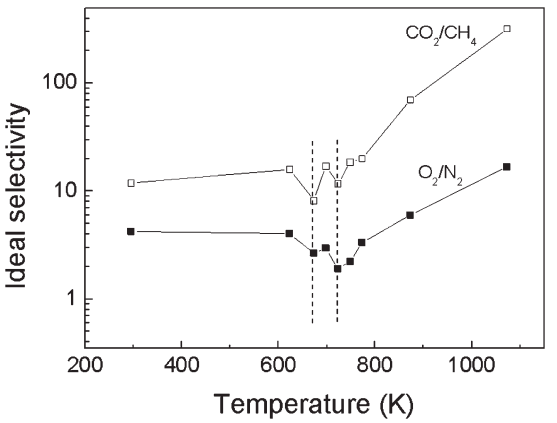

Figure 8 Ideal selectivities for the polyimide membrane and the membranes heat treated at temperatures in the range of 623–1073 K.

significant increase in the gas permeance in Figure 7 and thereafter the sustained weight loss in the temperature range of 773–873 K gives rise to sharp increases in gas permeance.

Figure 8 shows the effect of heat-treatment temperature on the ideal selectivity (ratio of the pure gas permeances) for O_2/N_2 and CO_2/CH_4. Increasing temperature from 623 to 673 K decreases the ideal selectivity for both O_2/N_2 and CO_2/CH_4. At the treatment temperatures of 673 and 723 K, the minimum values of selectivity for CO_2/CH_4 and O_2/N_2 respectively, are shown. As a semicrystalline polyimide, Kapton film contains both amorphous and ordered regions, and the heat treatment around the glass transition temperature (673 K) may improve the concentration of CTCs and promote further ordering/packing of the polyimide chains.[24] Consequently, the chains in the ordered regions are capable of strong intermolecular interactions, reducing the *d*-spacing and may result in reduced permeation rate of the gas molecules.[25] The minimum ideal selectivities shown by the membranes heat treated at 673 and 723 K may have resulted from the enhanced chain mobility and the decreased *d*-spacing.[10] The values for the true density (ρ) as well as the specific volume (1/ρ) determined for the polyimide membrane and the derived membranes heat treated between 623 and 773 K are given in Figure 9. It could be seen that the two lowest values of density also occurred at the same temperatures of 673 and 723 K which brought about the two minimum ideal selectivities in Figure 8. The heat treatment may affect the concentration of CTCs which in turn may lead to changes in the polyimide chain packing patterns and the fractional free volume, and therefore bringing about changes in the true density and selectivity. Also in Figure 8, treatment temperatures higher than 723 K resulted in continuously increased ideal selectivities for O_2/N_2 and CO_2/CH_4. The selectivities of O_2/N_2 and CO_2/CH_4 are 6.01 and 70.01 for membrane heat treated at 873 K and 16.75 and 320 for membrane heat treated at 1073 K, respectively. As pores are considered to evolve due to the diffusion of the gaseous products during pyrolysis and significant weight loss occurs within a temperature range of 773–923 K for a heating rate of 0.5 K/min (Fig. 2), it may surmise that the penetrable pores in the membranes are mainly created during the early stage of decomposition. The increased crystallinity as observed from the Raman spectra (Fig. 4) and the XRD spectra (Fig. 3) analyses of the membrane heat treated at 1073 K may account for the sharp decreases in the gas permeances from those of 873 K membranes (Fig. 7): the carbon developing into a more compact structure that is nearly impermeable for the gas molecules although the pyrolysis is in progress and far from completion. The decreased pore volume determined by N_2 (77 K) adsorption (Fig. 5) is another proof of this suggested occurrence. It can also be deduced that the heat treatment at 1073 K leads to more pronounced shrinkage of wide pores as compared with the narrow pores, thereby improving the permselectivities (Fig. 8). It should be noted that some wide pores still exist in 873 and 1073 K membranes as shown in Figure 6. Based on the separation factors shown in Figure 8, most of the mesopores may not exist as straight pores. Otherwise, the carbon membranes cannot give these separation factors. Consequently, most of the wide pores may not exist as straight pores. They may be connected through micropores, narrow channels between meso- and/or micropores, and the micropores predominantly control the transport properties of the carbon membranes.[26]

The membrane that was heat treated at 773 K showed higher gas permeances than the membranes heat treated at lower temperatures (Fig. 7) but all of

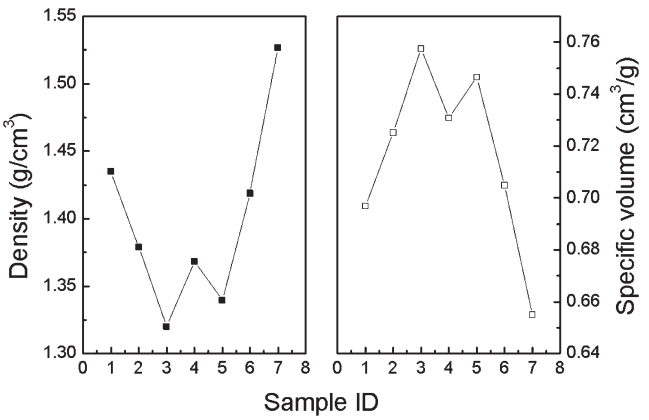

Figure 9 Densities and specific volumes of the polyimide membrane (1) and the membranes heat treated at temperatures in the range of 623, 673, 698, 723, 748, and 773 K (2–7).

them had comparable selectivities (Fig. 8). These properties may be attributed to the decomposition of the polyimide when subjected to heat treatment at various temperatures. Thus, the membrane heat treated at 773 K has an intermediate structure exhibiting properties of both polymeric material and amorphous carbon. The change in the selectivity shown by the membranes obtained at 673–748 K in Figure 8 is also an indication of the structural change upon heat treatment. The current study cannot directly prove the possible variations such as the concentration of CTCs, the chain mobility, the amorphousness, and the crystallinity of the polyimide membrane undergoing heat treatment at temperatures ranging from 673 to 773 K. Further study is needed to investigate the influences of heat treatment at 673–773 K on the physicochemical properties as well as the structure of the Kapton polyimide and the separation characteristics of the resulting carbon membranes.

CONCLUSIONS

The evolution of the structural and transport properties from Kapton polyimide membrane to carbon membrane upon heat treatment was investigated. In the temperature range of 673–748 K, the heat-treated polyimide membranes showed similar XRD patterns to that of the precursor, in terms of its semicrystalline structure. Two minimum ideal selectivities were observed for CO_2/CH_4 and O_2/N_2 at the heat-treatment temperatures of 673 and 723 K, respectively. Processing the polyimide membranes at temperatures higher than the glass transition temperature (673 K) but lower than 773 K for possible decomposition, the structural variation might be attributed to the change in the chain mobility and the concentration of CTCs. The membranes heat treated at 773 K showed appreciably higher gas permeances but comparable ideal selectivities when compared with the membranes processed at lower temperatures. The membranes heat treated at 873 and 1073 K showed typical XRD patterns of amorphous carbon, decreased *d*-spacing, and larger crystalline size. These structural changes exhibited very attractive molecular sieving properties which were superior to those of the precursor and the membranes heat treated at 623–773 K. Converting polyimide membrane to carbon membrane by heat treatment at 1073 K, the membrane selectivities for O_2/N_2 and CO_2/CH_4 improved from 4.23 to 16.75 and from 11.90 to 320, respectively.

References

1. Kusakabe, K.; Yamamoto, M.; Morooka, S. J Membr Sci 1998, 149, 59.
2. Fuertes, A. B.; Nevskaia, D. M.; Centeno, T. A. Micropor Mesopor Mater 1999, 33, 115.
3. Suda, H.; Haraya, K. J Chem Soc Chem Commun 1995, 1179.
4. Way, J. D.; Roberts, D. L. Sep Sci Technol 1992, 27, 29.
5. Shiflett, M. B.; Foley, H. C. Science 1999, 285, 1902.
6. Suda, H.; Haraya, K. J Phys Chem B 1997, 101, 3988.
7. Geiszler, V. C.; Koros, W. J Ind Eng Chem Res 1996, 35, 2999.
8. Tin, P. S.; Chung, T. S.; Kawi, S.; Guiver, M. D. Micropor Mesopor Mater 2004, 73, 151.
9. Barsema, J. N.; Klijnstra, S. D.; Balster, J. H.; Van der Vegt, N. F. A.; Koops, G. H.; Wessling, M. J Membr Sci 2004, 238, 93.
10. Shao, L.; Chung, T. S.; Pramoda, K. P. Micropor Mesopor Mater 2005, 84, 59.
11. Lua, A. C.; Su, J. C. Carbon 2006, 44, 2964.
12. Rao, M. B.; Sircar, S. J Membr Sci 1993, 85, 253.
13. Konno, H.; Nakahashi, T.; Inagaki, M. Carbon 1997, 35, 669.
14. Konno, H.; Shiba, K.; Kaburagi, Y.; Hishiyama, Y.; Inagaki, M. Carbon 2001, 39, 1731.
15. Hatori, H.; Yamada, Y.; Shiraishi, M.; Yoshihara, M.; Kimura, T. Carbon 1996, 34, 201.
16. Inagaki, M.; Meng, L.; Ibuki, T.; Sakai, M.; Hishiyama, Y. Carbon 1991, 29, 1239.
17. Jones, C. W.; Koros, W. J. Carbon 1994, 32, 1419.
18. Schwan, J.; Ulrich, S.; Batori, V.; Ehrhardt, H. J Appl Phys 1996, 80, 440.
19. Subramanyam, S. V.; Sayeed, A.; Meenakshi, V.; Bhattacharya, S.; Cholli, A.; Tripathi, S. J Appl Phys 1997, 81, 2907.
20. Ferrari, A. C.; Robertson, J. Phys Rev B 2000, 61, 14095.
21. Matthews, M. J.; Pimenta, M. A.; Dresselhaus, G.; Dresselhaus, M. S.; Endo, M. Phys Rev 1999, 59, 6585.
22. Yan, X. B.; Xu, T.; Wang, X. B.; Liu, H. W.; Yang, S. R. Surf Coat Technol 2005, 190, 206.
23. Gregg, S. J.; Sing, K. S. W. The Physical Adsorption of Gases by Microporous Solids: The Type I Isotherm in Adsorption Surface Area and Porosity; Academic Press: San Diego, 1997.
24. Feger, C.; Franke, H. In Polyimides: Fundamentals and Applications; Ghosh, M. K.; Mittal, K. L., Eds.; Marcel Dekker: New York, 1996.
25. Dunson, D. L. Ph.D. Thesis, Virginia Polytechnic Institute, 2000.
26. Zhou, W. L.; Yoshino, M.; Kita, H.; Okamoto, K. J Membr Sci 2003, 217, 55.